

CONDENSATION MASS TRANSFER IN UNSATURATED HUMID AIR INSIDE  
TUBULAR SOLAR STILL

By

Amimul Ahsan

Dept. of Architecture and Civil Engineering, University of Fukui, 3-9-1 Bunkyo, Fukui 910-8507, Japan

and

Teruyuki Fukuhara

Dept. of Architecture and Civil Engineering, University of Fukui, 3-9-1 Bunkyo, Fukui 910-8507, Japan

SYNOPSIS

A production model of a Tubular Solar Still based on a film-wise condensation theory that takes into account thermal resistance in unsaturated humid air inside a still is developed in this study. The condensation coefficient due to thermal resistance is inversely proportional to the dry air pressure fraction. In the present model, the overall heat transfer coefficient between the humid air inside the still and the ambient air outside the still is used for the first time because the measurement of the ambient air temperature is easier to obtain than the inner surface temperature of the tubular cover. The analytical solution of this condensation theory was able to yield a good agreement with the observed production flux obtained from this laboratory experiment. Furthermore, in order to assess the model's accuracy, the model's prediction is compared with field experimental data, proving that the model can be used to precisely predict the production flux.

INTRODUCTION

Solar distillation may be one of the most viable options for providing drinking water for a single house or a small community in an arid or coastal region. A solar still can be easily built on-site without using special tools. This easy assembly helps to shorten the transportation distance of the water from the still to the point of use. A basin type still is the most popular among solar stills, but is difficult to quickly repair and also to construct. A new type of solar distillation called a Tubular Solar Still (TSS) was designed by the authors' group to overcome the problems with the maintenance and management of the still. The TSS consists of a transparent tubular cover made of vinyl chloride and a trough inside the cover. Consequently, the weight of the TSS becomes much lighter than that of the basin type with a typical glass cover.

Many researchers (Chaibi (1), Clark (2), Hongfei et al. (3) and Shawaqfeh and Farid (4)) have proposed production models of the basin type still using evaporative heat and mass transfer correlations to predict the distilled water output, i.e. production. The distilled water is, however, produced after the condensation which takes place on

the inner surface of the tubular cover, following the evaporation from the water surface in a trough as shown in Fig. 1. Therefore, a time lag exists between the beginning of the production of distilled water and the occurrence of the evaporation (Islam (5)). By observing the time lag in the evaporation  $\rightarrow$  condensation  $\rightarrow$  production process in the still, we deduced that the theory of condensation may yield better results by predicting the hourly production than the past evaporation theories.

Many condensation theories (Yang et al. (6), Revankar and Pollock (7) and Raach and Mitrovic (8)) have been applied to a film flow achieved on a plate or a tube that derive the condensate mass flow and the heat transfer rate. However, the condensation theory for solar stills has not been fully examined compared with the other evaporation theories, because the data of the temperature and relative humidity of humid air is inadequate. We recently found that the relative humidity of the humid air was clearly not saturated (50-95%) in the daytime from our field experiments (Islam et al. (9) and Nagai et al. (10)). From these experiments, the condensate mass transfer coefficient was obtained empirically, but the theoretical expression was not fully developed.

This paper proposes a production model based on a film-wise condensation theory that takes into account the thermal resistance of unsaturated humid air. Furthermore, this work will attempt to show the validity of the proposed condensation theory by comparing the field experimental results of hourly production with the theoretical predictions.

## CONDENSATION THEORY OF TSS

### *Momentum and energy equations*

The following assumptions are made to simplify the analysis:

1. The TSS is cylindrical and set horizontally.
2. The condensate liquid film (liquid film) is a laminar flow and flows only along the inner circumference of the tubular cover, i.e. in the angular ( $\theta$ ) direction shown in Fig. 2.
3. The liquid film is a single homogeneous flow in the axial ( $x$ ) direction shown in Fig. 3(a).
4. The mean temperatures of the humid air and of the tubular cover (inner surface) are expressed as  $T_{ha}$  and  $T_{ci}$ , respectively.
5. The heat transfer at the liquid film-humid air interface (interface) is caused only by condensation. The

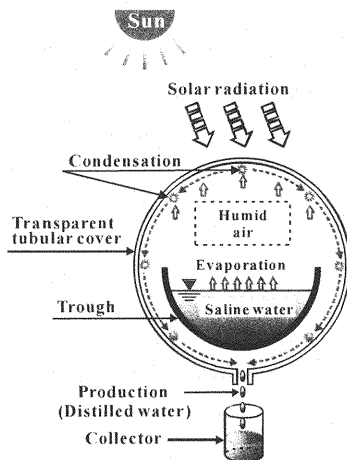


Fig. 1 Production mechanism of TSS

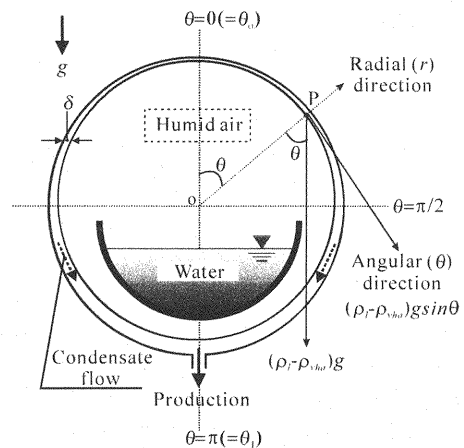


Fig. 2 Condensate liquid film flowing on the inner surface of the tubular cover and component of gravity force at point P

convection in the liquid film associated with the angular velocity,  $v_\theta$  does not contribute to the heat transfer in the liquid film.

6. The boundary layer of  $T_{ha}$  exists on the interface and the boundary layer thickness,  $\delta_{ha}$ , or the surface temperature of the liquid film,  $T_{ha}'$ , might be affected by the thermal resistance associated with the presence of a non-condensable gas (dry air) in the humid air (see Fig. 3(b)).
7. The interfacial shear stress at the interface is negligible, i.e.  $\tau_{i\theta} = 0$ .
8. The velocity ( $v_\theta$ ) gradient in the  $\theta$  direction is negligible compared to the radial ( $r$ ) direction.

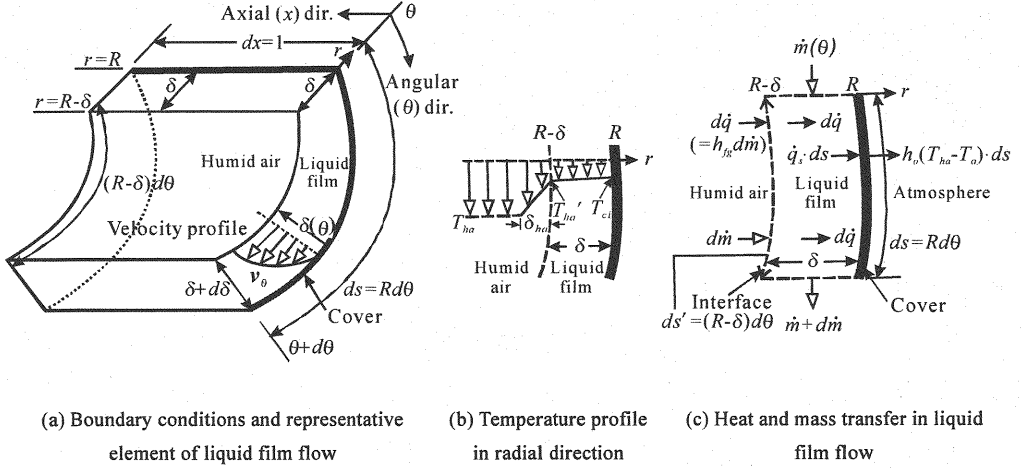


Fig. 3 Boundary conditions and heat and mass transfer in liquid film flow

Then the governing equations of momentum and energy for a liquid film under a steady state condition can be simplified as follows:

Momentum equation:

$$\left( \frac{d^2 v_\theta}{dr^2} + \frac{1}{r} \frac{dv_\theta}{dr} - \frac{v_\theta}{r^2} \right) + \frac{g}{\mu_l} (\rho_l - \rho_{vha}) \sin \theta = 0 \quad (1)$$

Energy equation:

$$\frac{d^2 T}{dr^2} + \frac{1}{r} \frac{dT}{dr} = 0 \quad (2)$$

The governing equations are subjected to the following boundary conditions:

$$v_\theta = 0; T = T_{ci} \text{ at } r = R, 0 \leq \theta \leq \pi \quad (3)$$

$$\tau_{i\theta} = \mu_l \left[ r \frac{d}{dr} \left( \frac{v_\theta}{r} \right) \right] = 0; T = T_{ha}' \text{ at } r = R - \delta(\theta), 0 \leq \theta \leq \pi \quad (4)$$

where,  $g$  = gravitational acceleration;  $\mu_l$  = dynamic viscosity of the condensate liquid;  $\rho_l$  = density of the condensate liquid;  $\rho_{vha}$  = density of water vapor in the humid air;  $R$  = radius of the TSS; and  $\delta$  = condensate film thickness. When integrating Eq. 1 is subjected to the boundary conditions of Eqs. 3 and 4, the profile of  $v_\theta$  in the  $r$  direction becomes

$$v_\theta = \left[ \frac{XR}{3} + \frac{X(R-\delta)^3}{6R^2} \right] r - \frac{X(R-\delta)^3}{6r} - \frac{Xr^2}{3} \quad (5)$$

where,  $X = \frac{g}{\mu_l} (\rho_l - \rho_{vha}) \sin \theta$ .

By using Fourier's law, the substantial heat flux for the neat area of the liquid film,  $q_s$ , at the interface ( $r=R-\delta$ ) is given by

$$q_s = -\lambda_l \left. \frac{dT}{dr} \right|_{r=R-\delta} \quad (6)$$

where,  $\lambda_l$  = thermal conductivity of the condensate liquid.

Integrating Eq. 2 subjected to the boundary conditions,  $T = T_{ci} \big|_{r=R}$  and  $T = T_{ha} \big|_{r=R-\delta}$ , yields

$$\left. \frac{dT}{dr} \right|_{r=R-\delta} = \frac{T_{ha} - T_{ci}}{(R-\delta) \ln \left( \frac{R}{R-\delta} \right)} \quad (7)$$

Substituting Eq. 7 into Eq. 6,  $q_s$  is given by

$$q_s = \frac{\gamma_l \lambda_l (T_{ha} - T_{ci})}{(R-\delta) \ln \left( \frac{R}{R-\delta} \right)} \quad (8)$$

where,  $\gamma_l = \frac{T_{ha} - T_{ci}}{T_{ha} - T_{ci}} (<1)$ .  $\gamma_l$  is called the temperature correction coefficient, which might be affected by the thermal resistance at the interface.

Since the liquid film thickness is fairly small compared to the radius of the TSS (i.e.  $\delta \ll R$ ), Eq. 8 is approximated as

$$q_s = \frac{\gamma_l \lambda_l (T_{ha} - T_{ci})}{\delta(\theta)} \quad (9)$$

The apparent heat flux for the whole area of the tubular cover,  $\dot{q}_s$ , can be expressed by using Eq. 9 as

$$\dot{q}_s = q_s \gamma_2 = \frac{\gamma_c \lambda_l (T_{ha} - T_{ci})}{\delta(\theta)} \quad (10)$$

where,  $\gamma_2$  ( $<1$ ) is the area fraction (=net area of the liquid film/whole area of the tubular cover) and might be influenced by the wettability of the cover material.  $\gamma_c$  ( $=\gamma_1/\gamma_2$ ) is called the condensation coefficient.

Based on the assumption 5., we know that the heat flow across the interface per unit length ( $dx=1$ ) due to condensation is equal to that across the inner surface of the tubular cover shown in Fig. 3(c). That is,

$$d\dot{q} = h_{fg} d\dot{m} = \dot{q}_s \cdot ds \quad (11)$$

where,  $\dot{q}$  = heat flow per unit length;  $h_{fg}$  = latent heat of vaporization;  $\dot{m}$  = condensate mass flow per unit length; and  $s$  = wetted perimeter. Using  $ds=Rd\theta$  and Eq. 11,  $\dot{q}_s$  is written as

$$\dot{q}_s = h_{fg} \frac{d\dot{m}}{Rd\theta} = h_{fg} \frac{d\dot{m}}{d\delta} \frac{d\delta}{Rd\theta} \quad (12)$$

*Condensate liquid film thickness*

$\dot{m}(\theta)$  can be obtained by the following integration:

$$\dot{m}(\theta) = \int_{R-\delta}^R \rho_l v_\theta dr \quad (13)$$

Substituting Eq. 5 into Eq. 13 yields

$$\dot{m}(\theta) = \frac{\rho_l X \delta^3}{3} = \frac{g \rho_l (\rho_l - \rho_{vha}) \delta^3 \sin \theta}{3 \mu_l} \quad (14)$$

Differentiating Eq. 14 in terms of  $\delta$  yields

$$\frac{d\dot{m}}{d\delta} = \frac{g \rho_l (\rho_l - \rho_{vha}) \delta^2 \sin \theta}{\mu_l} \quad (15)$$

Substituting Eqs. 10 and 15 into Eq. 12, the following relation is derived.

$$\delta^3 d\delta = \frac{\gamma_c \lambda_l \mu_l D (T_{ha} - T_{cl})}{2g \rho_l (\rho_l - \rho_{vha}) h_{fg}} \frac{d\theta}{\sin \theta} = A \frac{d\theta}{\sin \theta} \quad (16)$$

where,  $A = \frac{\gamma_c \lambda_l \mu_l D (T_{ha} - T_{cl})}{2g \rho_l (\rho_l - \rho_{vha}) h_{fg}}$ ; and  $D=2R$ .

Integrating Eq. 16 subjected to the boundary condition,  $\delta=0$  at top of the tubular cover, i.e.  $\theta=\theta_o$  ( $\approx 0$ ), yields the variation of  $\delta$  in the  $\theta$  direction,

$$\delta(\theta) = \left[ 4A \ln \left| \frac{\tan \theta / 2}{\tan \theta_o / 2} \right| \right]^{1/4} \quad (17)$$

*Heat transfer coefficient of unsaturated humid air*

$\dot{q}_s$  can be also expressed by using the local heat transfer coefficient of a liquid film,  $h_l$ , in the form

$$\dot{q}_s = h_l (T_{ha} - T_{cl}) \quad (18)$$

Substituting Eq. 10 into Eq. 18,  $h_l$  is given as

$$h_l = \frac{\gamma_c \lambda_l}{\delta(\theta)} \quad (19)$$

Substituting Eq. 17 into Eq. 19 yields

$$h_l = \gamma_c \lambda_l \left[ 4A \ln \left| \frac{\tan \theta / 2}{\tan \theta_o / 2} \right| \right]^{-1/4} \quad (20)$$

The average heat transfer coefficient,  $h_c$ , is defined as (see Fig. 2)

$$h_c = \frac{1}{(\theta_1 - \theta_o)} \int_{\theta_o}^{\theta_1} h_l d\theta \quad (21)$$

Since  $\theta_o=0^\circ$  cannot be applied to the integration of Eq. 21 because  $0^\circ$  cannot be calculated,  $\theta_o=1^\circ$  and  $\theta_1=180^\circ$  are chosen in this study. Thus,  $h_c$  is,

$$h_c = 0.996 \gamma_c^{\frac{3}{4}} \left[ \frac{g \rho_l (\rho_l - \rho_{vha}) h_{fg} \lambda_l^3}{\mu_l D (T_{ha} - T_{cl})} \right]^{1/4} \quad (22)$$

However, Eq. 22 is not practical because the measurement of  $T_{cl}$  is not as easy to obtain, compared to the measurement of the water surface temperature,  $T_w$ , the ambient air temperature,  $T_a$ , and  $T_{ha}$ . We, therefore, propose a new overall heat transfer coefficient,  $h_o$ , defined by the following equation:

$$h_o (T_{ha} - T_a) = h_c (T_{ha} - T_{cl}) \quad (23)$$

Eq. 23 means that the heat flux across the tubular cover is given by the product of  $h_o$  and the difference in temperature between the inside and outside of the TSS, i.e.  $T_{ha}-T_a$ .

Supposing that the temperature difference fraction,  $a=(T_{ha}-T_{cl})/(T_{ha}-T_a)$ , is constant,  $h_o$  is expressed as

$$h_o = 0.996 \gamma_c^3 \left[ \frac{g \rho_l (\rho_l - \rho_{vha}) h_{fg} a^3 \lambda_l^3}{\mu_l D (T_{ha} - T_a)} \right]^{1/4} \quad (24)$$

Thus, the condensate mass flux,  $m$ , is defined as

$$m = h_o (T_{ha} - T_a) / h_{fg} \quad (25)$$

Substituting Eq. 24 into Eq. 25,  $\gamma_c$  is given by

$$\gamma_c = \left( \frac{m}{0.996} \right)^{4/3} \left[ \frac{\mu_l D h_{fg}^3}{g \rho_l (\rho_l - \rho_{vha}) a^3 \lambda_l^3 (T_{ha} - T_a)^3} \right]^{1/3} \quad (26)$$

## EXPERIMENTAL METHOD AND CONDITIONS

### Laboratory experiments<sup>5)</sup>

To find the properties of  $\gamma_c$  and  $a$ , our laboratory experimental results are cited in this paper. Laboratory experiments on the productivity of a TSS were conducted in a thermostatic room to maintain a constant ambient air temperature and a relative humidity. The equipment consisted of a TSS, a solar simulator, two electric balances, a data logger and two computers. The TSS composed of a tubular cover and a semicircular black trough. The tubular cover used in the experiment was made of a curled transparent vinyl chloride sheet of 0.5mm in thickness. The length and outside diameter of the TSS were 0.52m and 0.13m, respectively. The trough was made of vinyl chloride with 1.0mm in thickness, 0.1m in outside diameter and 0.49m in length. Production was enhanced by using 12

Table 1 Laboratory experimental conditions and observed steady state values

Case	Experimental conditions			Observed values	
No.	$R_s$ (W/m <sup>2</sup> )	$T_a$ (°C)	$RH_a$ (%)	$T_{ha}$ (°C)	$RH_{ha}$ (%)
1	1200	35.3	35	66.1	78
2		32.1		63.4	78
3		26.6		59.4	77
4		22.2		59.8	73
5		17.0		55.2	72
6	800	35.3	35	58.2	81
7		32.0		55.6	81
8		26.5		51.6	81
9		22.4		51.0	76
10		16.2		46.9	75
11	500	35.1	35	50.7	85
12		31.7		47.6	86
13		26.5		42.8	86
14		22.7		39.2	90
15		17.0		33.9	90

infrared lamps (125W). The radiant heat flux,  $R_s$ , was controlled by changing the height of the lamps. The temperatures ( $T_{ha}$ ,  $T_{ci}$  and  $T_a$ ), the relative humidity of the humid air,  $RH_{ha}$ , and  $R_s$  were measured by means of thermo-couples, a thermo-hygrometer and a pyranometer, respectively. All the data were automatically recorded into a data logger and computers at one-minute intervals.

Table 1 shows the conditions of the laboratory experiments. The production was measured at three different levels of  $R_s$  and five different  $T_a$ , respectively.

#### Field experiments<sup>9)</sup>

Our field experimental results are cited to support the validity of the condensation theory. The same specifications mentioned in the section above for the TSS were drawn up for the field experiments.

## RESULTS AND DISCUSSIONS

### Laboratory experiments

Fig. 4 shows the relation between  $T_{ha}-T_{ci}$  and  $T_{ha}-T_a$ . As can be seen from the straight regression line, the value of  $a$  in Eq. 26 is 0.375. Since the condensation rate was not measured,  $\gamma_c$  was calculated by Eq. 26 under the assumption that the condensation flux is equal to the production flux.

Since the humid air is clearly not saturated, it can be inferred that  $\gamma_c$  is affected by the thermal resistance due to the presence of dry air. Based on this concept, Fig. 5 shows the relation between  $\gamma_c$  and the dry air pressure fraction,  $e_a/e_o$  (=partial dry air pressure/total atmospheric pressure). The value of  $\gamma_c$  is inversely proportional to  $e_a/e_o$  and the regression can be given as

$$\gamma_c = 0.0005 - 0.00046 \frac{e_a}{e_o} \quad (27)$$

where  $\frac{e_a}{e_o} = 1 - \frac{e_{vha}}{e_o}$ ;  $e_{vha} = f(T_{ha}, RH_{ha})$ .

Substituting Eq. 27 and  $a=0.375$  into Eq. 26,  $h_o$  in Eq. 25 is expressed by

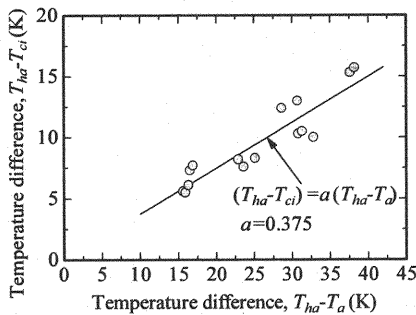


Fig. 4 Relation between temperature difference,  $T_{ha}-T_{ci}$ , and temperature difference,  $T_{ha}-T_a$ .

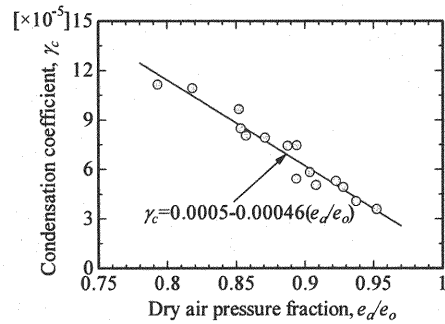


Fig. 5 Relation between condensation coefficient,  $\gamma_c$ , and dry air pressure fraction,  $e_a/e_o$ .



$$h_o = \left( 1.86 - 1.72 \frac{e_a}{e_o} \right)^{\frac{3}{4}} \left[ \frac{g \rho_l (\rho_l - \rho_{vha}) h_{fg} \lambda_l^3}{\mu_l D (T_{ha} - T_a)} \right]^{\frac{1}{4}} \times 10^{-3} \quad (28)$$

The hourly condensation mass flux,  $m_h$ , is defined as

$$m_h = \frac{3600 h_o (T_{ha} - T_a)}{h_{fg}} \quad (29)$$

Fig. 6 shows a comparison of  $m_h$  calculated by Eq. 29 with the observed hourly production flux,  $p_h$ . Eq. 29 corresponds precisely with the observed  $p_h$ .

#### Field experiments

Fig. 7 shows the observed diurnal variations of  $T_{ha}$ ,  $T_a$  and  $RH_{ha}$  obtained in Fukui, Japan on September 29th and October 6th, 2005. The temperature,  $T_{ha}$  rose rapidly after sunrise (approximately 6:00) and peaked between 12:00 and 13:00 on both days. The value of  $RH_{ha}$  was significantly below 100% in the daytime (minimum 50%) but about 100% during the night.

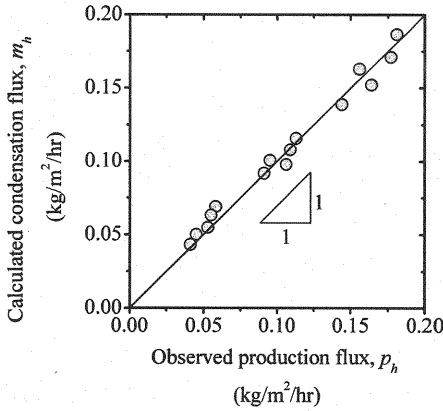


Fig. 6 Comparison of calculated condensation flux,  $m_h$ , with observed production flux,  $p_h$ .

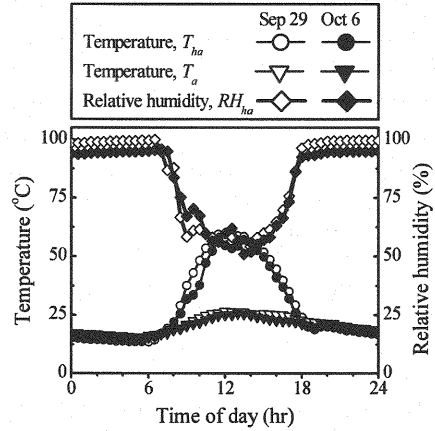


Fig. 7 Diurnal variations of temperatures and relative humidity obtained on September 29th and October 6th, 2005 in Fukui, Japan.

Fig. 8 shows the diurnal variations of  $p_h$  obtained from the field experiment and of  $m_h$  calculated by Eq. 29. The profile of the  $p_h$  is almost the same as that of the  $m_h$ . The time lag between the condensation and the production is negligible as far as the TSS used in the experiment is concerned.

Fig. 9 shows a comparison between the  $p_h$  and the  $m_h$ . Both correspond well with each other. From Figs. 8 and 9, it is revealed that the  $p_h$  can be substituted for  $m_h$ .

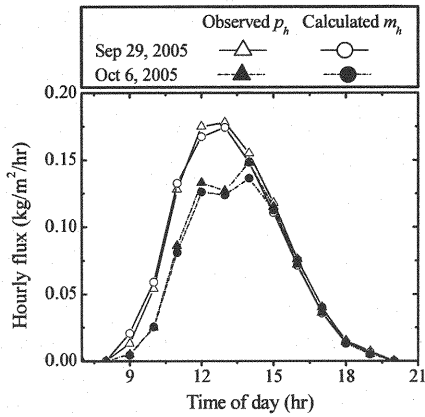


Fig. 8 Diurnal variations of observed production flux,  $p_h$ , and calculated condensation flux,  $m_h$ .

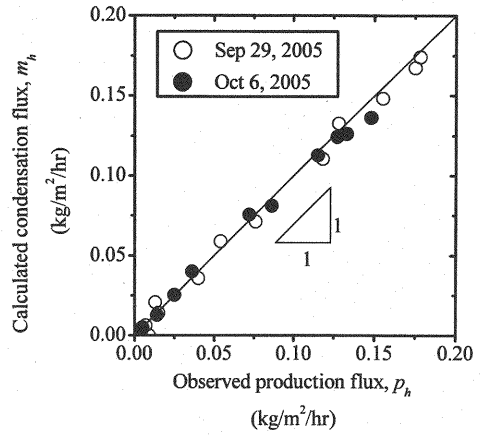


Fig. 9 Comparison of calculated condensation flux,  $m_h$ , with observed production flux,  $p_h$ .

## CONCLUSIONS

A production model of a Tubular Solar Still based on a film-wise condensation theory that takes into account of thermal resistance in unsaturated humid air inside the still is developed in this study. It was revealed that the condensation coefficient was in reverse proportion to the dry air pressure fraction. The present condensation theory using an overall heat transfer coefficient between humid and ambient air was able to yield a good agreement with the hourly production flux obtained from laboratory experiments. Moreover, the validity of the condensation theory was evaluated by making a comparison between the field experimental data and the theoretical results. Due to the correspondence of these results we concluded that the present condensation theory can be used to predict precisely the production flux of a TSS.

## REFERENCES

1. Chaibi, M. T.: Analysis by simulation of a solar still integrated in a greenhouse roof, *Desalination*, Vol.128, pp.123-138, 2000.
2. Clark, J. A.: The steady-state performance of a solar still, *Solar Energy*, Vol.44 (1), pp.43-49, 1990.
3. Hongfei, Z., Xiaoyan, Z., Jing, Z. and Yuyuan, W.: A group of improved heat and mass transfer correlations in solar stills, *Energy Con. & Mang.*, Vol.43, pp.2469-2478, 2002.
4. Shawaqfeh, A. T. and Farid, M. M.: New development in the theory of heat and mass transfer in solar stills, *Solar Energy*, Vol.55 (6), pp.527-535, 1995.
5. Islam, K. M. S.: Heat and vapor transfer in tubular solar still and its production performance, PhD thesis, Department of Architecture and Civil Engineering., University of Fukui, Japan, pp.33-52, 2006.
6. Yang, S. A., Li, G. C. and Yang, W. J.: Thermodynamic optimization of free convective film condensation on a horizontal elliptical tube with variable wall temperature, *Int. J. Heat & Mass Tran.*, Vol.50 (23-24), pp.4607-4613, 2007.

7. Revankar, S. T. and Pollock, D.: Laminar film condensation in a vertical tube in the presence of noncondensable gas, *App. Mathe. Modelling*, Vol.29, pp.341-359, 2005.
8. Raach, H. and Mitrovic, J.: Simulation of heat and mass transfer in a multi-effect distillation plant for sea water desalination, *Desalination*, Vol.204, pp.416-422, 2007.
9. Islam, K. M. S., Fukuhara, T. and Ahsan, A.: Tubular solar still-an alternative small scale fresh water management, *Proc. ICWFM-2007*, Bangladesh, pp.291-298, 2007.
10. Nagai, N., Takeuchi, M. et al.: Heat transfer modeling and field test on basin-type solar distillation device, *Proc. IDA World Cong.*, Bahrain, CD-ROM, BAH03-072, 2002.

#### APPENDIX-NOTATION

The following symbols are used in this paper:

$D$	= diameter of TSS (m);
$e_a$	= partial dry air pressure (Pa);
$e_o$	= total atmospheric pressure (101325 Pa);
$e_{vha}$	= partial water vapor pressure in humid air (Pa);
$g$	= gravitational acceleration (9.807 m/s <sup>2</sup> );
$h$	= heat transfer coefficient (W/m <sup>2</sup> ·K);
$h_{fg}$	= latent heat of vaporization (J/kg);
$\dot{m}$	= condensate mass flow per unit length (kg/m·s);
$m$	= condensation mass flux (kg/m <sup>2</sup> ·s);
$p_h$	= hourly production mass flux (kg/m <sup>2</sup> ·hr);
$\dot{q}$	= heat flow per unit length (W/m);
$q_s$	= substantial heat flux (W/m <sup>2</sup> );
$\dot{q}_s$	= apparent heat flux (W/m <sup>2</sup> );
$R$	= radius of TSS (m);
$R_s$	= radiative heat flux (W/m <sup>2</sup> );
$RH$	= relative humidity (%);
$s$	= wetted perimeter (m);
$T$	= temperature (K);
$T'$	= temperature of liquid film (K);

$v_\theta$	= angular velocity (m/s);
$\gamma_c$	= condensation coefficient (-);
$\gamma_t$	= temperature correction coefficient (-);
$\gamma_2$	= area fraction (-);
$\delta$	= condensate film thickness (m);
$\theta$	= azimuthal angle (radians);
$\lambda$	= thermal conductivity (W/m·K);
$\mu$	= dynamic viscosity (kg/m·s);
$\rho$	= density (kg/m <sup>3</sup> );
$\tau$	= shear stress (Pa);

*Subscripts*

$a$	= ambient air;
$c$	= condensation, condensate;
$ci$	= inner surface of tubular cover;
$h$	= hourly;
$ha$	= humid air;
$i\theta$	= interfacial shear stress in $\theta$ direction;
$l$	= condensate liquid, local;
$o$	= overall between humid and ambient air;
$vha$	= water vapor in humid air; and
$w$	= water surface.

(Received Jun 04, 2009 ; revised Dec 14, 2009)